Accepted Manuscript
Version of Record at: https://doi.org/10.1021/acssynbio.2c00502

A genetic engineering toolbox for the lignocellulolytic anaerobic gut fungus *Neocallimastix frontalis*

Casey A. Hooker[1,2], Radwa Hanafy[2], Ethan T. Hillman[1†], Javier Muñoz[1,3], and Kevin V. Solomon[1,2*]

[1]Department of Agricultural and Biological Engineering, Purdue University, West Lafayette, IN, 47907 USA

[2]Department of Chemical and Biomolecular Engineering, University of Delaware, Newark, DE, 19716 USA

[3]Department of Biomedical Engineering, Purdue University, West Lafayette, IN, 47907 USA

[†]Present Address: Department of Internal Medicine, University of Michigan Medical School, Ann Arbor, MI, 48109 USA

*Correspondence: kvs@udel.edu

Abstract

Anaerobic fungi are powerful platforms for biotechnology that remain unexploited due to a lack of genetic tools. These gut fungi encode the largest number of lignocellulolytic carbohydrate active enzymes (CAZymes) in the fungal kingdom, making them attractive for applications in renewable energy and sustainability. However, efforts to genetically modify anaerobic fungi have remained limited due to inefficient methods for DNA uptake and a lack of characterized genetic parts. We demonstrate that anaerobic fungi are naturally competent for DNA and leverage this to develop a nascent genetic toolbox informed by recently acquired genomes for transient transformation of anaerobic fungi. We validate multiple selectable markers (HygR and Neo), an anaerobic reporter protein (iRFP702), enolase and TEF1A promoters, TEF1A terminator, and a nuclear localization tag for protein compartmentalization. This work establishes novel methods to reliably transform the anaerobic fungus *Neocallimastix frontalis*, thereby paving the way for strain development and various synthetic biology applications.

Keywords: anaerobic gut fungi, transformation, parts, protein localization, gene expression, anaerobic reporter

Introduction

Anaerobic gut fungi (AGF; phylum Neocallimastigomycota), native to the digestive tracts of ruminant and hindgut animals, are primary colonizers of plant biomass that readily degrade crude lignocellulose.[1,2] Gut fungi thrive on a variety of complex plant materials ranging from crude C3 and C4 grasses, which differ in how carbon is fixed during photosynthesis, to untreated agricultural and forestry residues.[3] The ability of gut fungi to efficiently hydrolyze these feedstocks is proposed to be driven by the high diversity and abundance of carbohydrate active enzymes (CAZymes) encoded by their genomes.[4,5] The plethora of CAZymes, combined with the use of extracellular multienzyme lignocellulose-processing complexes or cellulosomes and the physical penetration of lignocellulosic biomass contribute to high lignocellulolytic activity.[5] Beyond applications in renewable energy technologies, anaerobic fungi may also be leveraged to identify new natural products as well as intermediates for drop-in biofuels. Multiple analyses of sequenced gut fungal genomes reveal an abundance of biosynthetic gene clusters encoding genes that produce uncharacterized natural products.[6–8] Together, anaerobic fungi offer a wealth of biotechnological potential that is only beginning to be realized.[9]

Efforts to characterize and tap into this biotechnological potential have revealed many proteins from anaerobic fungi that offer superior properties that are desirable for industrial processes.[10–12] These industrially relevant properties include thermostability, resistance to protease degradation, and preferential cofactor requirements, among others.[10,13] Additional efforts reveal signaling and/or transport proteins from gut fungi that may be leveraged as orthogonal systems in model organisms.[14–17] However, heterologous expression of many anaerobic fungal proteins remains challenging due to: 1) differences in host reducing conditions, which inhibits proper folding[18]; 2) a compositional bias towards amino acids encoded by AT-rich codons[13], which can present a metabolic burden that is not fully addressed by codon optimization[13,19], and 3) glycosylation and other post-translational modifications required for function that are not easily replicated in model hosts.[20] Consequently, developing genetic tools to manipulate AGF proteins in their native context will enable the discovery of novel anaerobic fungal genes and metabolic products of biotechnological importance.

Developing genetic tools and techniques to domesticate non-model organisms is an attractive strategy for building robust microbial cell factories.[21,22] These genetic toolkits at a minimum require efficient transformation schemes for introduction of nucleic acids, selectable markers and/or reporters to help validate transformation, and identification of constitutive promoters to drive expression of these genes[22]. With this preliminary set of genetic tools, additional parts such as terminator sequences, localization tags, replication sequences[23], and centromeric sequences[24] can be identified to enable stable expression, replication, and partitioning of genetic constructs *in vivo*.[25–27] Development of proper genetic tools enabling strain engineering efforts in anaerobic fungi has been hampered due to the fragmented nature of currently available genomes.[4,28,29] This high fragmentation is caused by shearing of the genome during lysis of the thick, chitin rich cell walls[28], extremely high genomic AT content that is challenging to assemble[4,30], and large homopolymeric sequences that impede genome assembly and thus annotation.[4,30] Beyond genome assembly and annotation, additional challenges are introduced by the complex lifestyle and life cycle of gut

69 fungi.[2,31] Anaerobic fungal life cycles begin with a motile flagellated zoospore stage that subsequently
70 attaches and encysts into plant biomass to initiate a non-motile phase characterized by sporangia and
71 rhizomycelia.[2] This complex alternating lifecycle coupled with an obligate anaerobic nature hinder the use
72 of traditional transformation methods such as *Agrobacterium tumefaciens* mediated transformation [32,33]
73 (ATMT), and protoplast-mediated transformation (PT), that are commonly used in aerobic fungi. ATMT does
74 not occur above 29 °C, well below the growth temperature of anaerobic fungi at 39 °C.[32] Moreover, the thick
75 chitin and glucan rich cell walls of anaerobic fungi significantly impede the efficacy of lytic enzymes
76 commonly used in protoplast-mediated transformations. Despite these challenges, they are not
77 insurmountable and there have been limited reports of transient anaerobic fungal transformation.

78 The feasibility of anaerobic fungal nucleic acid transformation was first demonstrated with harsh
79 biolistic bombardment of fungal biomass to introduce and transiently express a β-glucuronidase (GUS)
80 reporter gene.[34] While promising results were achieved, this delivery method resulted in high rates of cell
81 mortality and low transformation efficiencies (~4 transformants/μg DNA), and relied on isolation of fungal
82 zoospores in preparing cultures for transformation. Thus, gentler, higher throughput methods are needed
83 to reliably transform and domesticate anaerobic fungi. More recently, it was demonstrated that germinating
84 zoospores naturally uptake foreign, short RNA sequences (~21 bases).[35] This natural competency was
85 exploited to deliver small interfering RNA (siRNA) targeting the D-lactate dehydrogenase (*ldh*) gene,
86 significantly reducing gene expression and thus production of D-lactate. While delivery of siRNAs via natural
87 competency enabled higher cell survival rates, this protocol is limited to AGF species that can produce a
88 high concentration of zoospores. However, zoospore quantity is greatly affected by culture age, anaerobic
89 fungal species, and cultivation conditions. Thus, more efficient transformation strategies, particularly those
90 that enable uptake of larger nucleic acids and those that are not limited to a specific lifecycle stage are
91 greatly needed to improve transformation of gut fungi

92 In this work we establish transformation of anaerobic fungi with deoxyribonucleic acids (DNA) that
93 exploits the natural competency of their cells at multiple lifecycle stages. This approach removes the need
94 to enrich and selectively transform fungal zoospores enabling higher-throughput transformation methods
95 for this unique phylum of fungi. Using a novel AGF isolate from giraffe, *Neocallimastix frontalis* var *giraffae*
96 (Gf-ma), as a model system, we leverage our transformation protocol to evaluate the functionality of two
97 promoter sequences, multiple reporter constructs, and several selectable markers. We demonstrate that
98 coupling these selectable markers to anaerobic fluorophores enables screening of promoter activity and
99 monitoring of protein expression profiles *in vivo*. We also develop flow cytometry protocols to screen and
100 quantify transformation efficiency of these genetic constructs in fungal cells. Lastly, we have identified and
101 verified functionality of a nuclear localization signal sequence to enable targeting of proteins to anaerobic
102 fungal nuclei, which will be essential for future strain development efforts via gene editing technologies.
103 The methods and genetic tools developed here provide a framework for future synthetic biology and
104 functional genomic studies to leverage anaerobic fungi for their diverse biotechnological potential.
105
106

Results

Anaerobic fungi naturally take up DNA

As the first step for transformation, we needed to establish robust and efficient methods for DNA uptake. Prior biolistic methods were low efficiency with high cell mortality[34], while natural competency based methods were only established for short RNA sequences.[35] We first assessed whether anaerobic fungi were naturally competent for DNA and whether this ability was independent of life cycle stage (motile and vegetative). We generated short 50 nt dsDNA probes via primer annealing that we subsequently labeled with Cy3 fluorescent dye and mixed with young cultures (~18 h) of Gf-ma. Cy3 labeled DNA was rapidly taken up by multiple life stages of anaerobic fungi and observed in motile zoospores, vegetative sporangia, sporangiophores, and to a limited extent in rhizomycelia immediately after mixing (Figure 1). Within 60 minutes the Cy3-labeled DNA localized to the nucleus, suggesting that natural competence is a potential delivery vehicle for heterologous gene expression. More importantly, however, these results establish that anaerobic fungi are naturally competent for DNA at all lifecycle stages, obviating the need for time-consuming enrichment of zoospores as in previous methods.[34,35]

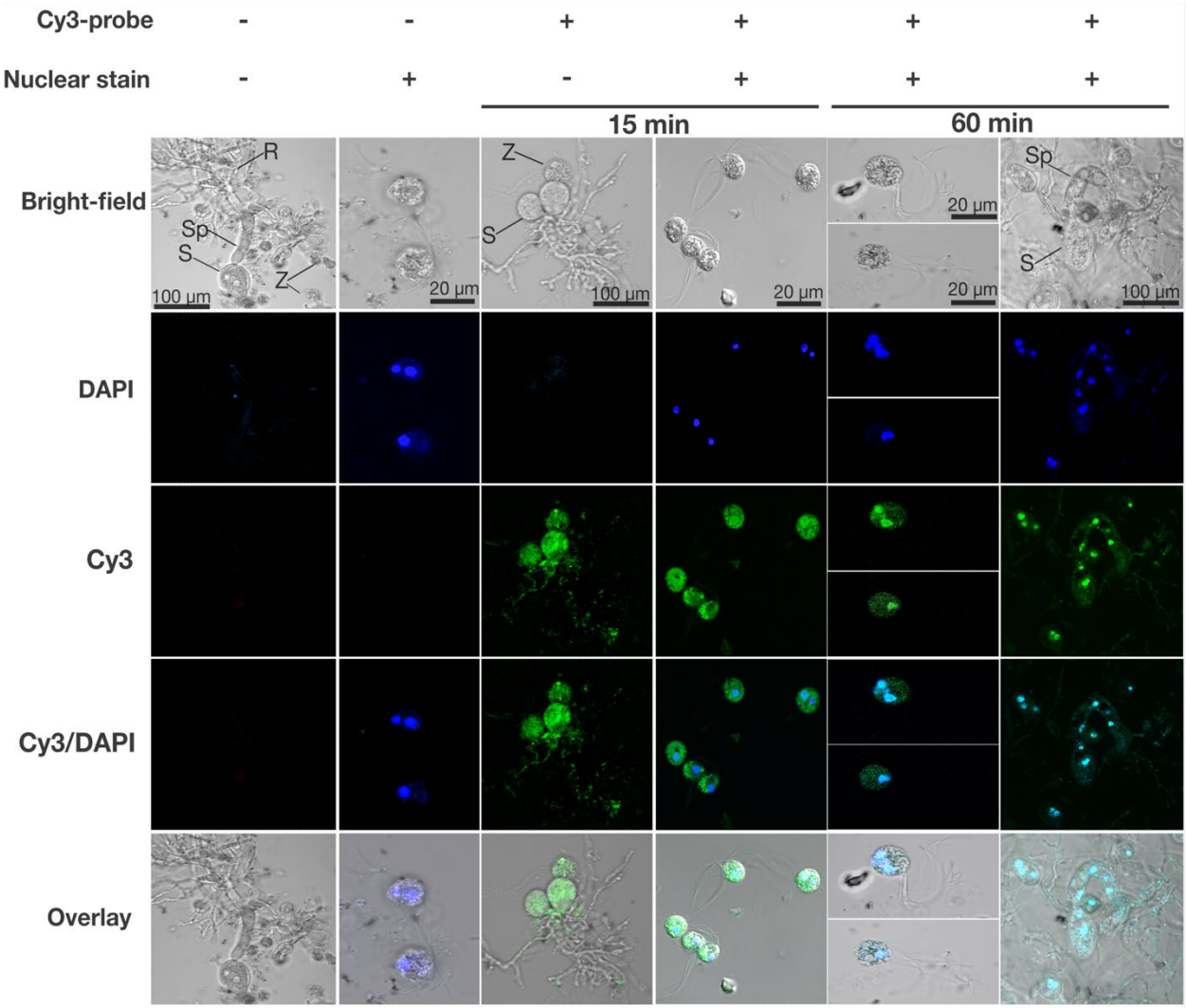

Figure 1: *Neocallimastix frontalis* var *giraffae* is competent for DNA, which localizes to the nucleus
Bright-field micrographs of fungal rhizomycelia (R), sporangia (S), sporangiophores (Sp), and zoospores (Z). Counterstaining Gf-Ma cells with DAPI reveal fungal nuclei. Cy3 channel visualization of fungal cells reveal sporangia and zoospores readily take up Cy3 labelled nucleic acid probes. Merging of DAPI and Cy3 channels show nucleic acid probes localize to nuclei of motile zoospores and vegetative sporangia.

Transformation efficiency via natural competency was then established via flow cytometry (Figure 2). The arithmetic mean of Cy3 fluorescence as measured with a phycoerythrin (PE) filter set increased 60% in transformed cells relative to untransformed controls (Figure 2; transformed population = $3.0 \pm 1.9 \times 10^4$ AU; untransformed population = $1.9 \pm 0.9 \times 10^4$ AU). This increase in fluorescence was statistically significant (unpaired t-test p-val $< 2.2 \times 10^{-16}$), suggesting significant uptake of DNA within the assayed cells. To calculate a minimum transformation efficiency, we counted the fraction of cells within the transformed population whose fluorescence was at least 2 standard deviations greater than the mean of the untransformed control group (i.e., statistically significant with $p \leq 0.05$). At least 16.5% of all observed cells were transformed with short nucleic acid probes (>40 transformants/μg DNA). However, these estimates are a conservative estimate or lower bound for transformation efficiency. To prevent clogging of the instrument only smaller zoospores (< 40 μm) were analyzed, excluding transformed sporangia and sporangiophores, which are too large to be run through a flow cytometer (Figure 1). Nonetheless, the flow cytometry independently confirmed DNA uptake via natural competency that could facilitate heterologous gene expression.

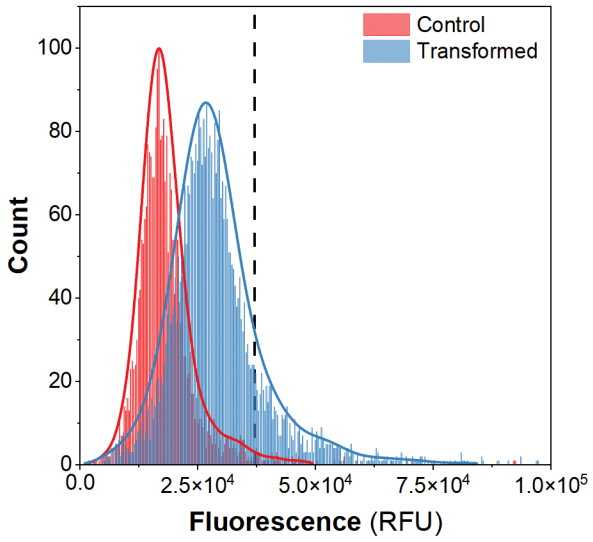

Figure 2: Flow cytometry of fungal zoospores for tracking DNA uptake efficiency
Cy3 fluorescence of gated events measured on the PE channel show transformed zoospores have higher mean fluorescence than untransformed controls. Mean fluorescence + 2 standard deviations of the control (dashed line) is used as the threshold to define a transformant. (See Table S5 for additional statistics of flow cytometry analysis and Figure S9 for collected events and gates used).

Selection systems for anaerobic fungi

150 As proof of concept for heterologous gene expression, we next identified potential selectable
151 markers for anaerobic fungi and minimal inhibitory concentrations (MIC) of frequently used antibiotics for
152 selection. Fungal growth was tracked by pressure over a multiple log concentration range (Figure 3).[36]
153 Hygromycin, geneticin (G418), neomycin, puromycin, and blasticidin strongly inhibited AGF growth with
154 varying levels of sensitivity (Table 1). AGF were weakly sensitive to neomycin with concentrations in excess
155 of 200 µg/ml needed to knock down growth (Figure 3C). This result is not unexpected as most fungi are not
156 susceptible to aminoglycosides except at high concentrations.[37] Puromycin and blasticidin were highly
157 lethal to AGF with no growth under the concentrations tested (MIC < 3 µg/ml; Figure 3D-E). However, AGF
158 were moderately sensitive to hygromycin and G418 with MICs of 5 and 10 µg/ml, respectively. Conversely,
159 AGF are resistant to bleomycin with no growth inhibition at concentrations of up to 50 µg/ml bleomycin
160 (Figure 3F). Subsequent genome analysis of all sequenced AGF confirmed the presence of a conserved
161 bleomycin resistance gene (lactoglutathione lyase- *lgl*), which forms part of the glyoxyl detoxification
162 pathway.[38,39] This pathway is responsible for protecting hosts from oxidative stress[40,41], which would be
163 evolutionarily advantageous for anaerobic fungi in their native environment. Thus, this resistance gene may
164 serve as a convenient counter-selectable marker for future genome engineering efforts. Given their clear
165 and reproducible MICs, relatively low cost, and high sensitivity, hygromycin and G418 selection were used
166 to establish heterologous expression in anaerobic fungi.

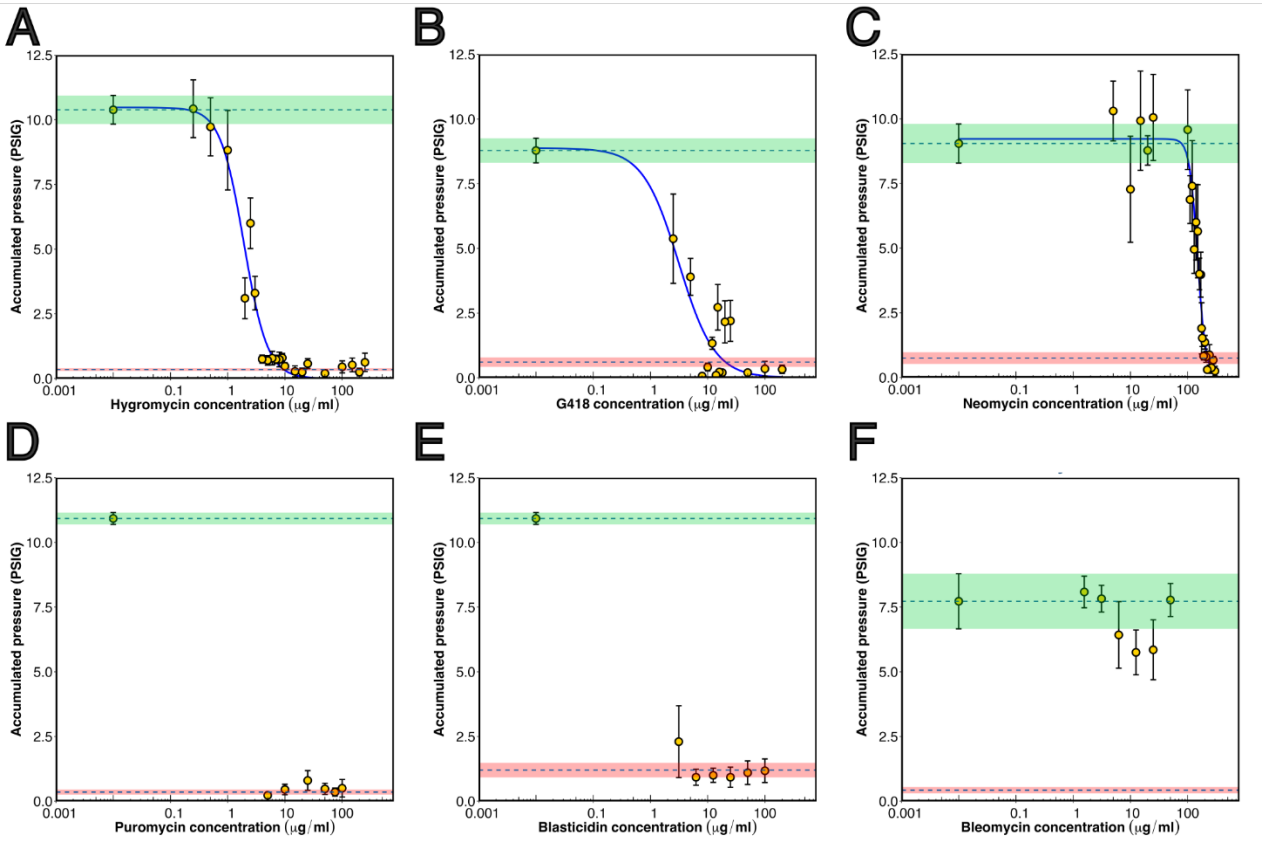

167
168 **Figure 3: *Neocallimastix frontalis* var *giraffae* is susceptible to hygromycin (A), G418 (B) Neomycin**
169 **(C), Puromycin (D), Blasticidin (E), but not Bleomycin (F)**. N ≥ 4 biological replicates. Error bars

170 represent standard error of the mean. Dashed lines represent the average pressure of uninoculated tubes
171 (lower line) or positive control (upper line) while the red ribbon represents the standard error of the
172 uninoculated controls and the green ribbons represents the standard error of the positive control.
173

174 **Table 1: Minimal Inhibitory Concentrations of Tested Antibiotics**

Antibiotic	Mechanism	MIC (µg/ml)
Blasticidin-S	Inhibits translation	<3
Bleomycin	Induced DNA breaks	Not detected
Geneticin (G418)	Inhibits translation	10
Hygromycin	Inhibits translation	5
Neomycin	Inhibits translation	200
Puromycin	Inhibits translation	<3

175

176 **Genetic parts for heterologous expression**

177 To develop a robust heterologous expression system in anaerobic fungi, we identified constitutive
178 promoters and transcriptional terminators from conserved non-coding upstream and downstream
179 sequences flanking highly conserved and highly expressed essential enolase (ENOL) and translation
180 elongation factor 1 alpha (TEF1A) genes. These two genes were constitutively expressed on seven different
181 carbon sources in evolutionarily related *Neocallimastix californiae* and *Piromyces finnis* isolates,[4] and due
182 to their essential nature in carbohydrate metabolism and amino acid biosynthesis hypothesized to express
183 at similarly constitutive levels in Gf-Ma. This analysis provided 2 putatively strong constitutive promoters,
184 P_{ENOL} and P_{TEF1A}, and 1 terminator, T_{TEF} terminator (see Supplementary text for details), which we used to
185 construct several heterologous gene cassettes with codon harmonized selectable markers (Hyg – *hph*;
186 G418 – *neo;* Table 2). Genes were codon harmonized (see Supplementary text for details) by selecting
187 AGF codons with relative abundances (Table S1) that matched those of the gene in their native hosts to
188 ensure high expression.

189 We then tested the ability of these genetic constructs to rescue fungal growth in the presence of
190 hygromycin or G418. As these genetic constructs lacked Autonomously Replicating Sequences (ARS) and
191 centromeric sequences (CEN) for replication and partitioning to daughter cells[42], we dosed in ~2 µg of
192 linearized plasmid daily (Figure 4A). Control studies with labelled plasmid confirmed that larger plasmid
193 DNA was also taken up and localized to the nucleus (Figure 4B and Figure S5), potentially enabling gene
194 expression. We transformed our cells with unlabeled DNA and grew them in non-selective media for 72 h
195 to express the selectable marker before subculturing in selective media (Figure 4A). Cells without construct
196 showed negligible growth (pressure accumulation) when grown in the presence of antibiotic (Figures 4C
197 and D). Cells transformed with P_{ENOL}-*hph* cassettes were able to grow to similar levels above the construct-
198 free negative control in selective media ($p = 0.005$; Figure 4C, Table 2) with significant levels of biomass
199 generation. However, this growth was only ~60% of positive (non-selective) control levels ($p = 0.001$) as
200 measured by pressure evolution (Figure 4C and Figure S6A). These effects are only observed with regular
201 dosing of exogenous DNA (data not shown); that is, provided DNA constructs do not persist in the absence
202 of stabilizing sequences such as an ARS. Similarly, the P_{TEF1A}-*neo* construct was able to rescue ~75% of

growth relative to positive (non-selective) controls (Figure 4D). Promoter-less control constructs (pUCM6-AGF-124) do not rescue growth in selective media and are indistinguishable from untransformed negative controls (Figure S7). Antibiotic resistance phenotypes are dependent on our cloned upstream regions validating that they contain constitutive promoters that are active in anaerobic fungi and can drive heterologous gene expression.

To facilitate the development of gene editing tools and future approaches for more stable transformations, we identified nuclear localization sequences (NLS) that could be used to traffic Cas endonucleases and/or other enzymes to the nucleus. Analysis of the leader sequence of nuclear-localized histone H2B across multiple fungal lineages revealed strong conservation in the first 40 amino acids of anerobic fungal histone proteins (Figure 5A, and Dataset SD5)[5,39,43–45]. This region was distinct from that of homologs in other fungal lineages forming an AGF-specific putative NLS. The AGF consensus sequence (Figure 5B, and Dataset SD6) was used to flank an anaerobic fluorescent reporter protein, iRFP702[46,47], which we codon-optimized for anaerobic fungi. We also generated control reporter constructs that lacked NLS sequences. All reporter constructs were also fused to hygromycin selection cassettes to enable enrichment of transformed cells in selective media. Cells transformed with reporter plasmids all exhibited increased far-red fluorescence as visualized by confocal microscopy and strong fungal growth under selective conditions (Figure 5C; Figure S6A). Expression was observed in all fungal life cycle stages examined. While NLS-free constructs showed more diffuse fluorescence, constructs flanked by NLS sequences displayed punctate or localized fluorescence that coincided with stained nuclei. In other words, addition of the NLS sequence did not disrupt fluorescence of the iRFP fluorophore and, more importantly, localized iRFP to fungal nuclei. To quantify this phenomenon, transformed cells were analyzed via flow cytometry. The arithmetic mean fluorescence of transformed cells lacking the NLS sequence was 3.50 times as much as that of untransformed cells (Figure 6). NLS-tagged transformants exhibited 4.55 times the fluorescence of untransformed controls, potentially due to the localized or concentrated nature of protein expression (Figure 6). In summary, we successfully identified and validated anaerobic fluorescent reporters and NLS sequences for AGF establishing powerful new tools to track protein expression and localize proteins to specific compartments.

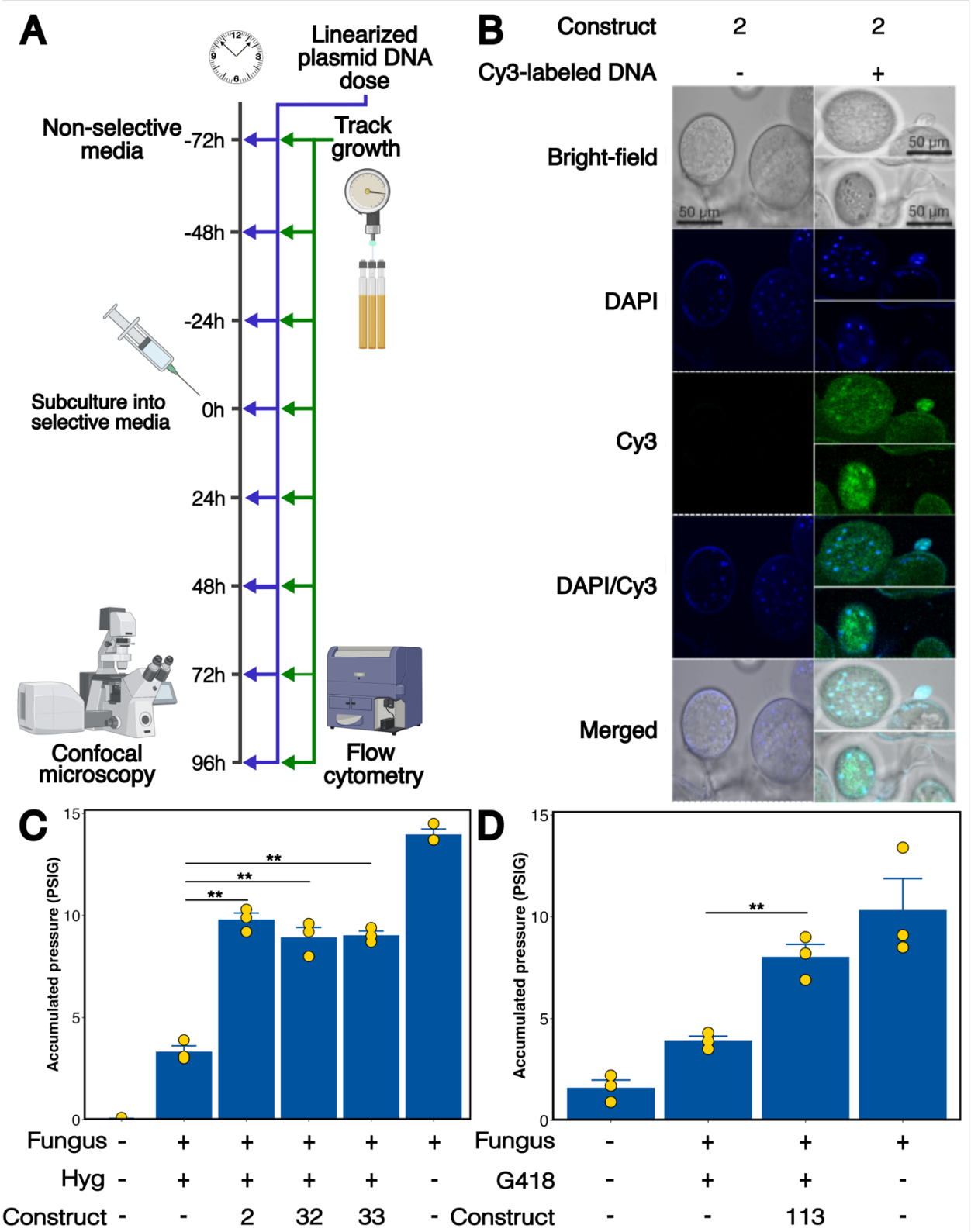

Figure 4: Dosing linearized plasmids into *Neocallimastix frontalis* var *giraffae* rescues fungal growth under selective conditions. A) Plasmid dosing scheme B) Cy3 labelled pUCM6-AGF-2 harboring P_{ENOL}-*hph* is taken up and localizes to fungal nuclei C) Hygromycin resistance markers can be heterologously

expressed and rescue growth in selective media relative to untransformed control via P_{ENOL} [Constructs express: 2 – Hyg^R, 32 – Hyg^R + a nuclear localized fluorescent reporter, 33 – Hyg^R + fluorescent reporter] D) *neo* resistance marker is heterologously expressed from P_{TEF1A} in construct 113 to rescue growth on G418. See Table 2 for a full description of each construct and Figure S6 for corresponding growth curves. ** p-value ≤ 0.0050

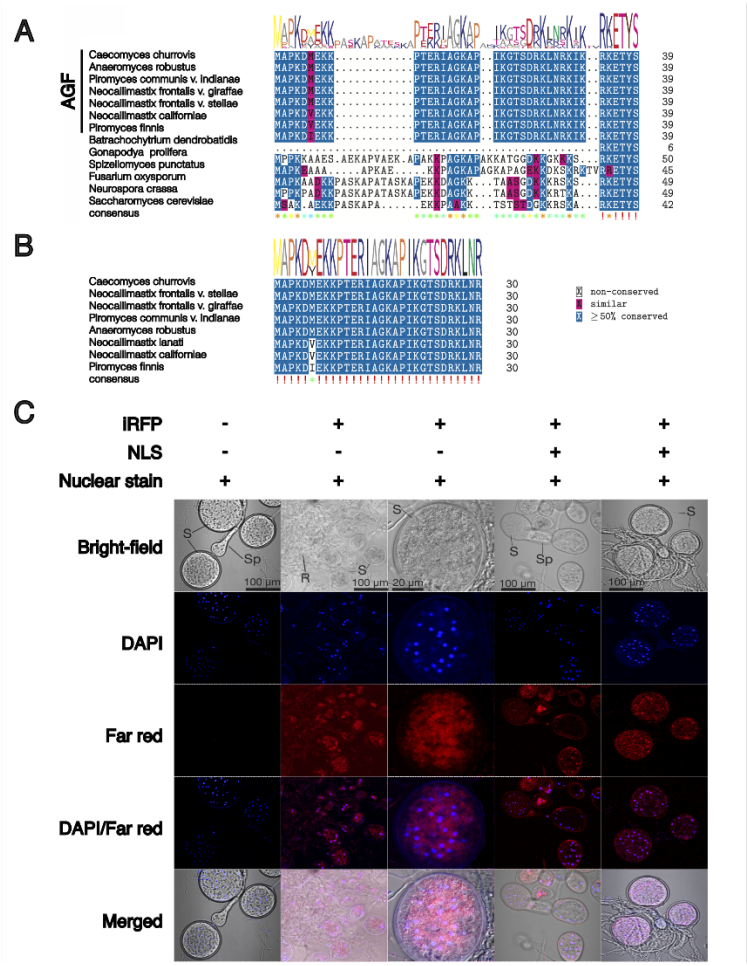

Figure 5: NLS sequence from Histone H2B localizes anaerobic fluorescent reporters to the nuclei of fungal cells. A) Anaerobic fungi have unique 5' leader sequences on histone H2B that are distinct from leader sequences of model fungal lineages. B) Consensus sequence of conserved anaerobic fungi Histone 2B leader sequence or putative NLS. C) Confocal microscopy of fungal cells transformed with constructs containing hygromycin resistance and iRFP enable selection and visualization of iRFP expression. See Table 2 for full descriptions of these constructs.

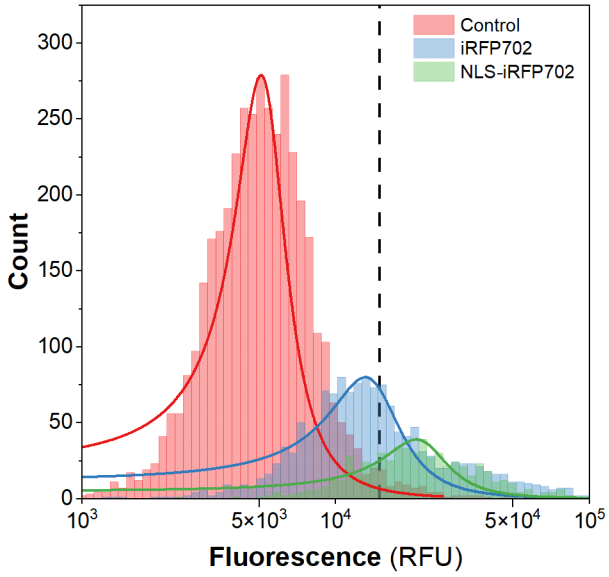

250
251 **Figure 6: Flow cytometry analysis of fungal cells transformed with iRFP cassettes** Fluorescence for
252 gated events of fungal zoospores transformed with iRFP containing constructs have a higher mean
253 fluorescence (2.0 x 10^5) than untransformed controls (5.8 x 10^4). Similarly, fluorescence for gated events
254 of zoospores transformed with NLS-tagged iRFP also show higher mean fluorescence (2.6 x 10^5) than
255 untransformed controls. Table 2 contains full descriptions of the constructs used to generate these plots,
256 and Table S5 provides additional details on collection of flow cytometry data. Raw flow cytometry data and
257 gates used provided in Figure S10
258
259 **Discussion**
260 Anaerobic fungi offer a wealth of biotechnological potential such as superior enzymes to hydrolyze
261 plant biomass[4], or previously unidentified natural products [6,8], however efforts to domesticate and engineer
262 these organisms has significantly lagged behind that of many emerging model organisms. Methods and
263 tools to transform model fungal lineages relying on protoplasting or *Agrobacterium* mediated protocols[32]
264 are not amenable to anaerobic fungi due to the thick cell wall and differences in cultivation temperature. In
265 this work we establish natural competency as a robust scheme to introduce DNA into fungal cells (Figure
266 1). Natural competency has been reported in model fungal lineages as a strategy by which nucleic acids
267 can be reliably introduced. While natural competency for RNA has been reported and leveraged for RNAi
268 silencing in anaerobic fungi[35], our work demonstrates that DNA competency can be similarly exploited for
269 heterologous expression. This approach is less lethal than previous biolistic methods[34], the only previously
270 demonstrated method for DNA transformation of anaerobic fungi, and is at least 10 times more efficient
271 than that of previously reported biolistic methods (~40 transformants/µg vs < 4 transformants/µg via biolistic
272 methods).[34]. Moreover, this approach is more accessible to labs, removing the need for specialized
273 equipment such as an anaerobic chamber to manipulate the fungi. All that is needed are sealed Hungate
274 tubes to cultivate anaerobic fungi and syringes to inoculate and introduce DNA. Further, our transformation
275 scheme also expands on past natural competency transformation methods by transforming all lifecycle
276 stages instead of selectively transforming anaerobic fungal zoospores.[35] By transforming all lifecycle stages

277 instead of enriching only fungal zoospores we are able to perform transformations approximately 72 hours
278 faster than currently reported methods, significantly reducing the Design Build Test Learn cycle.
279 Additionally, we established the first methods for performing flow cytometry of anaerobic fungal zoospores
280 (Figure 2 and Figure 6) which not only enables rapid screening of transformants, but also establishes a
281 procedure for estimating transformation efficiency. In summary, our scheme for transforming anaerobic
282 fungi overcomes past bottlenecks of high cell mortality, high cost, and low throughput.

283 In this work we also establish a suite of genetic parts to enable genetic engineering of gut fungi
284 including promoters, resistance markers, nuclear localization sequences, and fluorescent reporters. To date
285 the only functional genetic parts identified for anaerobic fungi were the enolase promoter of *Neocallimastix*
286 *frontalis* and the enzymatic reporter β-glucoronidase[34]. However, as this was developed before community
287 repositories such as Addgene and the source isolate lost, no genetic parts are currently available for these
288 organisms. To address this lack of parts, we identified and validated functionality of two promoter
289 sequences (Figures S1-S2, Figure 4C-D) and demonstrated that they reliably drive expression of two
290 antibiotic resistance markers, *hph* and *neo*. Moreover, we identified and validated functionality of an
291 anaerobic fungal NLS sequence (Figure 5A-B). This sequence was anaerobic fungal specific and, similarly
292 to those found on other histone proteins in other species, did not display a classical monopartite or bipartite
293 structure.[48] Anaerobic fungal genomes are especially GC-poor leading to a depletion of amino acids
294 encoded by GC-rich codons such as arginine, which are common in NLSs.[48,49] Our identified NLS contained
295 no GC-rich codon repeats and was ~10 residues shorter than NLSs from later diverging fungi. Thus,
296 anaerobic fungi may have evolved unique nuclear importins that do not rely as strongly on canonical
297 arginine residues for function. Despite this, the identified NLS retains a net positive charge (pI ~ 10.1) under
298 homeostatic conditions, like canonical NLS sequences, suggesting some conserved mechanism for nuclear
299 transport.

300 We also validate the use of the anaerobic reporter iRFP in anaerobic fungi to visualize protein
301 trafficking within anaerobic fungi (Figure 5C) and leveraged this expression to develop flow cytometry
302 protocols to rapidly screen transformed populations (Figure 6). Transformants were 3-4x brighter than
303 control cells validating heterologous expression in specific cellular compartments. However, the low
304 brightness suggested low transformation or expression. While iRFP was selected in this study due to the
305 low background fluorescence of anaerobic fungi within its fluorescence spectra, it is a dim fluorophore with
306 a brightness (quantum yield × molar extinction) up to an order of magnitude lower than other anaerobic
307 fluorophores such as iLOV[46] and UnaG.[50] Thus, future studies should expand this palette of reporters to
308 improve the sensitivity of these tools and more robustly quantify transformation efficiency.

309 In this study, we have developed simple and reliable methodologies for the transformation of the
310 emerging anaerobic fungal chassis. We demonstrate that these species are naturally competent for DNA
311 during multiple stages of their life cycle and can heterologous express and traffic a number of enzymes and
312 reporters to various cellular compartments. While only transient, this transformation can be sustained
313 through periodic dosing of heterologous DNA directly to cell culture – no equipment or sample preparation

314 is required. More importantly, these methods are potentially enabling for future strain development efforts
315 such as those that use CRISPR technology. In many fungi and higher eukaryotes, transient expression is
316 optimal for gene editing due to toxicity arising from off-target events with high stable expression of Cas9.[51–
317 53] Use and further development of these tools unlocks new avenues of research in this class of
318 lignocellulolytic fungi, accelerating the development of these species for biomanufacturing,[12,54,55] drug
319 discovery[6,7] biogas,[56,57] and agriculture.[9]
320
321
322 **Methods:**
323 *Anaerobic fungal isolate, media and growth conditions:*
324 *Neocallimastix frontalis* var *giraffae* (Gf-ma) was isolated from the feces of a giraffe (*Giraffa*
325 *reticulata*) from the Indianapolis Zoo and maintained on a semi-defined medium B supplemented with
326 chloramphenicol at a final concentration of 35 µg/ml as previously described.[12] All cultures were grown in
327 14 ml Hungate tubes at 39 °C unless otherwise specified. Briefly, media was prepared by microwaving all
328 components except glucose and cysteine for approximately 13 minutes prior to sparging with CO_2 (Keen
329 Gas, Newark, DE, USA) for approximately 1 hour to remove oxygen present in the media. Subsequently,
330 glucose (5 g/l) (Fisher Scientific, Waltham, MA, USA) and L-Cysteine hydrochloride (1.25 g/l) (Fisher
331 Scientific, Waltham, MA, USA) were added prior to dispensing media into individual tubes. Specifically,
332 anaerobic liquid media was dispensed to 14 ml Hungate tubes or 100 ml serum bottles under 100% CO_2.
333 Anaerobic tubes and bottles were then sealed and maintained under 100% CO_2 headspace prior to
334 autoclaving with an exposure time of 20 minutes at 120 °C. Sterile anaerobic media was stored at 4 ºC until
335 it was ready for use. All media was prewarmed to 39 ºC one hour before inoculation. To assess the
336 phylogenetic affiliation of strain Gf-ma in relation to the other *Neocallimastix* species as well as other
337 anaerobic fungal genera, four copies of the D1/D2 of nuc 28S rDNA genes sequences were extracted from
338 the genome.[39] The obtained sequences were aligned to anaerobic fungal reference 28S rDNA sequence
339 dataset downloaded from the National Center for Biotechnology Information (NCBI) GenBank nr database
340 using Clustal W using default parameters and manually refined in MEGA7.[58] The generated alignment was
341 then used to construct a maximum likelihood phylogenetic tree in FastTree using the gtr model[59] with
342 *Chytriomyces* sp. WB235A as the outgroup. Bootstrap values were calculated based on 100 replicates
343 (Figure S8).
344
345 *Transformations of Neocallimastix. frontalis var giraffae with labeled nucleic acid probes:*
346 To assess the natural competency of strain Gf-ma to exogenous dsDNA, a 50 bp long ssDNA (5'-
347 ATCTGTACCGGCTAATGCGAATCGATAGCTACCGATTGCGATTCGGATTC-3') was purchased from
348 Integrated DNA Technologies, Inc.(Coralville, IA, USA) and labeled with Cyanine3 (Cy3) fluorescent dye at
349 the 5′ end to enable visual detection of DNA uptake. Cy3 labeling was conducted using *Label* IT™ nucleic
350 acid labeling kit, Cy3 from Mirus Bio (Madison, WI, USA) following the manufacturer's instructions. Then
351 we created a double stranded DNA probe by annealing the Cy3-labeled ssDNA oligomers with the
352 unlabeled complementary strand by incubating them at 95 °C followed by a gradual cooling down at room

353 temperature for 45 min to permit hybridization. Young cultures of strain Gf-ma (18 h, grown on medium B)
354 were mixed with Cy3-labeled dsDNA at a final concentration of 20 nM, and incubated at 39 °C for 90 min.
355 Samples were taken every 15 min., counterstained with 4′,6 diamidino-2-phenylindole (DAPI; 10 µg/mL)
356 and examined using confocal microscopy (see *Confocal Microscopy and Image processing*) for nuclear
357 visualization and detection of DNA uptake by different lifecycle stages. The Cy3 kit was also used to label
358 a heterologous construct harboring hygromycin resistance (See Figure 4B) following the same workflow.
359
360 *Kill curve assays*
361 To determine the minimal inhibitory concentration of antibiotics on *Neocallimastix*. *frontalis* var
362 *giraffae*, 14 ml Hungate tubes containing 9 ml of media B and chloramphenicol (see *Anaerobic fungal*
363 *isolate, media and growth conditions*) received either hygromycin B, neomycin, puromycin dihydrochloride,
364 blasticidin s hydrochloride, or G418. All antibiotic solutions were diluted in water to achieve 100X solutions
365 at each concentration range to be tested. 100 µl of 100X working solution was then added to each tube
366 prior to inoculation with 1 ml of actively growing *Neocallimastix frontalis* var *giraffae* culture. In order to
367 overcome biological noise, all test conditions as well as positive and negative controls were carried out in
368 biological quadruplicate at a minimum. Additionally, all Hungate tubes were zeroed out to atmospheric
369 pressure immediately after inoculation. Growth of *Neocallimastix frontalis* var *giraffae* was determined by
370 pressure accumulation [36] in the sealed Hungate tubes via a pressure transducer (Automation Products
371 Group, Logan, UT, USA) daily over a period of 7 days. Total accumulated pressure was then determined
372 for all test conditions. Growth curves of pressure accumulation versus antibiotic concentration were
373 generated in R with the ggplot2 package.[60] The pracma package was used to fit Hill equations to the data.[61]
374
375 *Transformations of Neocallimastix. frontalis var giraffae with reporter constructs on linearized plasmids*
376 Constructs tested in this report were first transformed into chemically competent *E. coli* strain DH5α.
377 Single colonies were inoculated into 5 ml of Lauria-Bertani (LB) broth containing 100 µg/ml ampicillin and
378 cultured at 37 ºC at 250 RPM. After approximately 16-18 hours, these 5 ml liquid cultures were used to
379 inoculate 50 ml LB cultures containing 100 ug/ml Ampicillin in 25 0ml baffled flasks. The 50 ml *E. coli*
380 cultures were incubated at 37 ºC at 250 RPM until the optical density reached approximately 2.5
381 absorbance units. Liquid cultures were subsequently centrifuged at 10,000 RCF for 10 minutes at 4 ºC prior
382 to midiprepping with a GeneJet midiprep kit (Fisher Scientific, Waltham, MA, USA). Midiprepped plasmid
383 DNA was linearized with Fast Digest BamHI or EcoRI in Fast Digest buffer. DNA digest reactions were heat
384 inactivated for 5 minutes at 80 ºC, according to the manufacturer's instructions. Sterile anaerobic water
385 (1.25 g/l cysteine hydrochloride, 1.5 g/l PIPES) was prepared in sterile 100 ml serum bottles and sparged
386 with CO_2 for five minutes to remove oxygen. Sterile anaerobic water was subsequently prewarmed to 39 ºC
387 and used to dilute digested DNA to a final volume of 300 µl. 100 µl of this digested DNA was added to each
388 Hungate tube so that all constructs were tested in biological triplicate. After addition of digested plasmid
389 DNA, Hungate tubes were zeroed to atmospheric pressure. Since these genetic constructs are unstable
390 due to the lack of Autonomously Replicating Sequences (ARS) and centromeric sequences (CEN), we

391 dosed in ~2 µg of linearized plasmid daily before and after antibiotics selection and fluorophore detection
392 (Figure 4A).
393
394 *Flow cytometry of Neocallimastix frontalis* var *giraffae cultures*
395 Fungal zoospores were collected from liquid cultures by opening Hungate tubes, filtering through
396 8 layers of cheesecloth directly into sterile 50ml Falcon tubes to remove large fungal biomass and
397 rhizomycelia while also enriching for fungal zoospores. This filtered fermentation liquor was then centrifuged
398 at 4,500 RCF for 10 minutes at 39 ºC to pellet fungal zoospores. The supernatant was gently decanted and
399 the resulting pellet was resuspended in 1 ml of sterile anaerobic water prewarmed to 39 ºC (See
400 *Transformations of Neocallimastix. frontalis* var *giraffae with reporter constructs on linearized plasmids*).
401 The concentrated zoospores were then carefully pipetted through BD FACS tubes with 35 µm mesh size
402 (BD, Franklin Lakes, NJ, USA) to eliminate any clumps or cell debris. Samples were immediately analyzed
403 using a NovoCyte flow cytometer. For flow cytometry analysis on Cy3 transformed cultures 50,000 ungated
404 events were collected with an opening of 21.1 µm and a flow rate of 104 µl per minute. A PE (R-
405 Phycoerythrin) laser with 488 nm excitation and 660/20 nm detection was used for all Cy3 transformed
406 fungal zoospores. Gating was performed by running media only controls to determine which events were
407 caused by debris in fungal media. For flow cytometry on cultures transformed with iRFP containing
408 constructs, the Alexa-Fluor 700 channel was used with 640 nm excitation and 695/40 nm detection with the
409 same flow rate and opening size. Gating of events was performed through the same procedure as Cy3
410 transformed zoospores. Fluorescence intensity on PE-H or Alexa Fluor 700-H was compared to
411 untransformed controls, and transformation efficiency was calculated by determining the number of gated
412 events having fluorescence signal at least 2 standard deviations above the mean fluorescence intensity of
413 untransformed controls. For all analyses, the arithmetic mean fluorescence was used when calculating
414 transformation efficiency. Data collection and analysis were performed with NovoExpress 1.5.0.
415
416 *Confocal microscopy and image processing*
417 Fungal biomass was harvested from liquid cultures and stained with 4,6′-diamidino-2-phenylindole
418 (DAPI; 10 µg/mL) to be scanned using confocal laser scanning microscopy (CLSM). Images were captured
419 using a Zeiss LSM 980/Airyscan 2 (Carl Zeiss, Inc., Gottingen, Germany), equipped with 40X and 60X oil
420 immersion objective lens. Fungal cells transformed with Cy3 were examined using a Cy3 (Cyanine-3)
421 channel applying the following wavelengths: 534 nm for excitation and 694 nm for detection. While fungal
422 cells transformed with iRFP were examined using Alexa-Fluor 700 channel applying the following
423 wavelengths: 640 nm for excitation and 755 nm for detection. Nuclear visualization and localization were
424 detected via a DAPI channel applying the following wavelengths: 410 nm for excitation and 605 nm for
425 detection. Image acquisition and processing were handled using an AxioCam and Fiji software[62].
426
427 *Promoter and terminator alignments*
428 DNA sequences for regions upstream of Neocallimastigomycota enolase genes were downloaded
429 from Mycocosm[39] and aligned in RStudio Version 4.2.0.[63] DNA sequences were aligned with the multiple

430 sequence alignment (MSA) package version 1.28.0 within the Bioconductor suite version 3.15.[64,65]
431 Sequences were aligned using ClustalW with the default substitution matrix, the neighbor joining method,
432 a gap open penalty of 15, and gap extension penalty of 6.6 with 3 iterations.[64] For all promoter alignments
433 5' untranslated sequences, if annotated, were included in the alignment. Terminator sequence alignments
434 were created using the same alignment parameters, however 3' untranslated sequences, if present in the
435 genome annotation, were excluded. All protein IDs used to create these alignments are presented in Tables
436 S1 and S2). Complete multiple sequence alignments for these analyses are available as Datasets SD1-
437 SD6.
438
439 *Identification of a Nuclear Localization Signal Sequence*
440 To identify a putative Nuclear Localization Signal (NLS) sequence in anaerobic fungi, amino acid
441 sequences of histone H2B, a protein that is targeted to the nuclei of eukaryotic cells, were collected from
442 Mycocosm.[39] This preliminary list included both species of fungi in the Neocallimastigomycota lineage as
443 well as model fungi (Figure 4A). Protein IDs collected from Mycocosm[39] from the corresponding genomes
444 are listed in Table S3. These sequences were aligned using the MSA R package within the Bioconductor
445 suite.[64,65] The histone H2B multiple sequence alignment files are available as Supplemental Dataset SD5
446 which includes both anaerobic fungal and model fungal lineages, and Dataset SD6 which only includes gut
447 fungal H2B sequences. The first 30 amino acids of histone H2B (protein ID 728204) for *Neocallimastix*
448 *frontalis* var *giraffae* were selected as an NLS and cloned on the 5' and 3' ends of an AGF codon
449 harmonized variant of iRFP702. 5X glycine linkers were used between NLS sequences and the iRFP702
450 gene. These NLS sequences were additionally codon harmonized to further promote expression when
451 transformed into anaerobic fungi. pUCM6-AGF-32, which contains the NLS tagged iRFP fluorophore, is
452 described in more detail in Table 2.
453
454 **Table 2: Description of constructs used in the present work.**

Construct ID	Plasmid Name	Relevant genoytpe	Size (bp)
2	pUCM6-AGF-2	ColE1(pBR322) ori, *bla*(Amp^r), P_{ENOL}-HygR(AGF-harmonized)-T_{TEF1A}	5465
32	pUCM6-AGF-32	ColE1(pBR322) ori, *bla*(Amp^r), P_{ENOL}-HygR(AGF-harmonized)-T_{TEF1A}-P_{ENOL}-NLS-iRFP702(AGF-harmonized)-NLS-T_{TEF1A}	7862
33	pUCM6-AGF-33	ColE1(pBR322) ori, *bla*(Amp^r), P_{ENOL}-HygR(AGF-harmonized)-T_{TEF1A}-P_{ENOL}-iRFP702(AGF-harmonized)-T_{TEF1A}	7628
79	pUCM6-AGF-79	ColE1(pBR322) ori, *bla*(Amp^r), P_{TEF1A}-HygR(AGF-harmonized)-T_{TEF1A}-P_{ENOL}-iRFP702(AGF-harmonized)-T_{TEF1A}	7633
113	pUCM6-AGF-113	ColE1(pBR322) ori, *bla*(Amp^r), P_{TEF1A}-Neo(AGF-optimized)-T_{TEF1A}	5252
124	pUCM6-AGF-124	ColE1(pBR322) ori, *bla*(Amp^r), HygR(AGF-harmonized)-T_{TEF1A}	5497

455
456

Supporting information

- Supplementary Info: Description of how anaerobic fungal parts were developed, information about sequences used in bioinformatic analyses, flow cytometry data, fungal growth curves, and phylogenetic analysis
- Dataset SD1: SD1_Enolase_1000_MSA.txt - alignment of anaerobic fungal enolase leader sequences used to identify an enolase promoter
- Dataset SD2: SD2_TEF1A_1000_Promoter_MSA.txt- alignment of Translation Elongation Factor 1 Alpha (TEF1A) leader sequences used to identify a TEF1A promoter for anaerobic fungi
- Dataset SD3: SD3_TEF1A_500_Terminator.txt - alignment of TEF1A downstream sequences used to identify a TEF1A terminator for anaerobic fungi
- Dataset SD4: SD4_Gfma_TEF1A_500_Terminator.txt - alignment of *Neocallimastix frontalis* TEF1A promoter sequences used to identify a *Neocallimastix frontalis* TEF1A promoter
- Dataset SD5: SD5_NLS_all_MSA.txt - alignment of fungal histone H2B sequences used to assess Nuclear Localization Signal sequence conservation across multiple fungal lineages
- Dataset SD6: SD6_Neocallimastigomycota_H2B.txt- alignment of anaerobic fungal histone H2B sequences to assess Nuclear Localization Signal sequence conservation across all Neocallimastigomycota

Conflicts of Interest

The authors declare no competing financial interest.

Author contributions

K.V.S conceived the study. EH performed strain isolation. C.H., E.H. J.M, and R.H. performed genomic analyses. CH, EH, and RH designed constructs generated in this study. C.H. and R.H. performed transformations in this study. R.H. performed confocal microscopy and image processing. C.H. performed flow cytometry experiments and analyses. C.H. and R.H. and K.V.S wrote the manuscript.

Acknowledgments

CH was supported by a National Science Foundation Graduate Research Fellowship under DGE-1333468. This material is based upon work supported by the U.S. Department of Energy, Office of Science, Office of Biological and Environmental Research under Award Number DE-SC0022018/DE-SC0022206 and the National Science Foundation under Grant No. IOS-2128272. A portion of this research was performed under the Facilities Integrating Collaborations for User Science (FICUS) program (proposal doi: 10.46936/fics.proj.2018.50397/60000049) and used resources at the DOE Joint Genome Institute (https://ror.org/04xm1d337) and the Environmental Molecular Sciences Laboratory (https://ror.org/04rc0xn13), which are DOE Office of Science User Facilities operated under Contract Nos. DE-AC02-05CH11231 (JGI) and DE-AC05-76RL01830 (EMSL). The LSM980 confocal microscope was acquired with a shared instrumentation grant (1S10RR027273-01) from the National Institutes of Health (NIH). Microscopy access was supported by grants from the NIH-NIGMS (P20 GM103446), the NIGMS (P20 GM139760) and the State of Delaware. This publication was made possible by the Delaware INBRE program, supported by a grant from the National Institute of General Medical Sciences – NIGMS (P20 GM103446) from the National Institutes of Health and the State of Delaware. Last, we would like to express our gratitude and pay our respects to the late Dr. Richard West for his considerable help in the Flow Cytometry Core facility.

References

(1) Gruninger, R. J.; Puniya, A. K.; Callaghan, T. M.; Edwards, J. E.; Youssef, N.; Dagar, S. S.; Fliegerova, K.; Griffith, G. W.; Forster, R.; Tsang, A.; McAllister, T.; Elshahed, M. S. Anaerobic Fungi (Phylum Neocallimastigomycota): Advances in Understanding Their Taxonomy, Life Cycle, Ecology, Role and Biotechnological Potential. *FEMS Microbiol. Ecol.* **2014**, *90* (1), 1–17. https://doi.org/10.1111/1574-6941.12383.

(2) Orpin, C. Studies on the Rumen Flagellate Neocallimastix Frontalis. *Microbiology* **1975**, *91* (2), 249–262. https://doi.org/10.1099/00221287-91-2-249.

(3) Hooker, C. A.; Hillman, E. T.; Overton, J. C.; Ortiz-Velez, A.; Schacht, M.; Hunnicutt, A.; Mosier, N. S.; Solomon, K. V. Hydrolysis of Untreated Lignocellulosic Feedstock Is Independent of S-Lignin Composition in Newly Classified Anaerobic Fungal Isolate, Piromyces Sp. UH3-1. *Biotechnol. Biofuels* **2018**, *11* (1), 293. https://doi.org/10.1186/s13068-018-1292-8.

(4) Solomon, K. V.; Haitjema, C. H.; Henske, J. K.; Gilmore, S. P.; Borges-Rivera, D.; Lipzen, A.; Brewer, H. M.; Purvine, S. O.; Wright, A. T.; Theodorou, M. K.; Grigoriev, I. V.; Regev, A.; Thompson, D. A.; O'Malley, M. A. Early-Branching Gut Fungi Possess a Large, Comprehensive Array of Biomass-Degrading Enzymes. *Science* **2016**, *351* (6278), 1192. https://doi.org/10.1126/science.aad1431.

(5) Haitjema, C. H.; Gilmore, S. P.; Henske, J. K.; Solomon, K. V.; de Groot, R.; Kuo, A.; Mondo, S. J.; Salamov, A. A.; LaButti, K.; Zhao, Z.; Chiniquy, J.; Barry, K.; Brewer, H. M.; Purvine, S. O.; Wright, A. T.; Hainaut, M.; Boxma, B.; van Alen, T.; Hackstein, J. H. P.; Henrissat, B.; Baker, S. E.; Grigoriev, I. V.; O'Malley, M. A. A Parts List for Fungal Cellulosomes Revealed by Comparative Genomics. *Nat. Microbiol.* **2017**, *2* (8), 17087. https://doi.org/10.1038/nmicrobiol.2017.87.

(6) Swift, C.L.; Louie, K.B.; Bowen, B. P.; Olson, H. M.; Purvine, S. O.; Salamov, A.; Mondo, S. J.; Solomon, K. V.; Wright, A. T.; Northen, T. R.; Grigoriev, I. V.; Keller, N. P.; O'Malley, M. A. Anaerobic Gut Fungi Are an Untapped Reservoir of Natural Products. *Proc. Natl. Acad. Sci.* **2021**, *118* (18), e2019855118. https://doi.org/10.1073/pnas.2019855118.

(7) Hillman, E. T.; Readnour, L. R.; Solomon, K. V. Exploiting the Natural Product Potential of Fungi with Integrated-Omics and Synthetic Biology Approaches. *Curr. Opin. Syst. Biol.* **2017**, *5*, 50–56. https://doi.org/10.1016/j.coisb.2017.07.010.

(8) Brown, J. L.; Swift, C. L.; Mondo, S. J.; Seppala, S.; Salamov, A.; Singan, V.; Henrissat, B.; Drula, E.; Henske, J. K.; Lee, S. Co-cultivation of the Anaerobic Fungus Caecomyces Churrovis with Methanobacterium Bryantii Enhances Transcription of Carbohydrate Binding Modules, Dockerins, and Pyruvate Formate Lyases on Specific Substrates. *Biotechnol. Biofuels* **2021**, *14* (1), 1–16. https://doi.org/10.1186/s13068-021-02083-w.

(9) Hooker, C. A.; Lee, K. Z.; Solomon, K. V. Leveraging Anaerobic Fungi for Biotechnology. *Curr. Opin. Biotechnol.* **2019**, *59*, 103–110. https://doi.org/10.1016/j.copbio.2019.03.013.

(10) Li, X.-L.; Ljungdahl, L. G.; Ximenes, E. A.; Chen, H.; Felix, C. R.; Cotta, M. A.; Dien, B. S. Properties of a Recombinant β-Glucosidase from Polycentric Anaerobic Fungus Orpinomyces PC-2 and Its Application for Cellulose Hydrolysis. *Appl. Biochem. Biotechnol.* **2004**, *113* (1), 233–250. https://doi.org/10.1385/abab:113:1-3:233.

(11) Seppälä, S.; Wilken, St. E.; Knop, D.; Solomon, K. V.; O'Malley, M. A. The Importance of Sourcing Enzymes from Non-Conventional Fungi for Metabolic Engineering and Biomass Breakdown. *Metab. Eng.* **2017**, *44*, 45–59. https://doi.org/10.1016/j.ymben.2017.09.008.

(12) Hillman, E. T.; Li, M.; Hooker, C. A.; Englaender, J. A.; Wheeldon, I.; Solomon, K. V. Hydrolysis of Lignocellulose by Anaerobic Fungi Produces Free Sugars and Organic Acids for Two-Stage Fine Chemical Production with Kluyveromyces Marxianus. *Biotechnol. Prog.* **2021**, *37* (5), e3172. https://doi.org/10.1002/btpr.3172.

(13) Hillman, E. T.; Frazier, E. M.; Shank, E. K.; Ortiz-Velez, A. N.; Englaender, J. A.; Solomon, K. V. Anaerobic Fungal Mevalonate Pathway Genomic Biases Lead to Heterologous Toxicity Underpredicted by Codon Adaptation Indices. *Microorganisms* **2021**, *9* (9), 1986. https://doi.org/10.3390/microorganisms9091986.

(14) Podolsky, I. A.; Seppälä, S.; Xu, H.; Jin, Y.-S.; O'Malley, M. A. A SWEET Surprise: Anaerobic Fungal Sugar Transporters and Chimeras Enhance Sugar Uptake in Yeast. *Metab. Eng.* **2021**, *66*, 137–147. https://doi.org/10.1016/j.ymben.2021.04.009.

(15) Podolsky, I. A.; Schauer, E. E.; Seppälä, S.; O'Malley, M. A. Identification of Novel Membrane Proteins for Improved Lignocellulose Conversion. *Curr. Opin. Biotechnol.* **2022**, *73*, 198–204. https://doi.org/10.1016/j.copbio.2021.08.010.

(16) Seppälä, S.; Yoo, J. I.; Yur, D.; O'Malley, M. A. Heterologous Transporters from Anaerobic Fungi Bolster Fluoride Tolerance in Saccharomyces Cerevisiae. *Metab. Eng. Commun.* **2019**, *9*, e00091. https://doi.org/10.1016/j.mec.2019.e00091.
(17) Yoo, J. I.; Seppälä, S.; O'Malley, M. A. Engineered Fluoride Sensitivity Enables Biocontainment and Selection of Genetically-Modified Yeasts. *Nat. Commun.* **2020**, *11* (1), 1–9. https://doi.org/10.1038/s41467-020-19271-1.
(18) Gasser, B.; Saloheimo, M.; Rinas, U.; Dragosits, M.; Rodríguez-Carmona, E.; Baumann, K.; Giuliani, M.; Parrilli, E.; Branduardi, P.; Lang, C.; Porro, D.; Ferrer, P.; Tutino, M. L.; Mattanovich, D.; Villaverde, A. Protein Folding and Conformational Stress in Microbial Cells Producing Recombinant Proteins: A Host Comparative Overview. *Microb. Cell Factories* **2008**, *7* (1), 11. https://doi.org/10.1186/1475-2859-7-11.
(19) Seppälä, S.; Lankiewicz, T. S.; Saxena, M.; Henske, J. K.; Salamov, A. A.; Grigoriev, I. V.; O'Malley, M. A. Genomic and Proteomic Biases Inform Metabolic Engineering Strategies for Anaerobic Fungi. *Metab. Eng. Commun.* **2020**, *10*, e00107. https://doi.org/10.1016/j.mec.2019.e00107.
(20) O'Malley, M. A.; Theodorou, M. K.; Kaiser, C. A. Evaluating Expression and Catalytic Activity of Anaerobic Fungal Fibrolytic Enzymes Native to Piromyces Sp E2 in Saccharomyces Cerevisiae. *Environ. Prog. Sustain. Energy* **2012**, *31* (1), 37–46. https://doi.org/10.1002/ep.10614.
(21) Riley, L. A.; Guss, A. M. Approaches to Genetic Tool Development for Rapid Domestication of Non-Model Microorganisms. *Biotechnol. Biofuels* **2021**, *14* (1), 30. https://doi.org/10.1186/s13068-020-01872-z.
(22) Fatma, Z.; Schultz, C.; Zhao, H. Recent Advances in Domesticating Non-model Microorganisms. *Biotechnol. Prog.* **2020**, e3008. https://doi.org/10.1002/btpr.3008.
(23) Nakamura, Y.; Nishi, T.; Noguchi, R.; Ito, Y.; Watanabe, T.; Nishiyama, T.; Aikawa, S.; Hasunuma, T.; Ishii, J.; Okubo, Y. A Stable, Autonomously Replicating Plasmid Vector Containing Pichia Pastoris Centromeric DNA. *Appl. Environ. Microbiol.* **2018**, *84* (15), e02882-17. https://doi.org/10.1128/AEM.02882-17.
(24) Cao, M.; Seetharam, A. S.; Severin, A. J.; Shao, Z. Rapid Isolation of Centromeres from Scheffersomyces Stipitis. *ACS Synth. Biol.* **2017**, *6* (11), 2028–2034. https://doi.org/10.1021/acssynbio.7b00166.
(25) Teh, M. Y.; Ooi, K. H.; Danny Teo, S. X.; Bin Mansoor, M. E.; Shaun Lim, W. Z.; Tan, M. H. An Expanded Synthetic Biology Toolkit for Gene Expression Control in Acetobacteraceae. *ACS Synth. Biol.* **2019**, *8* (4), 708–723. https://doi.org/10.1021/acssynbio.8b00168.
(26) Crozet, P.; Navarro, F. J.; Willmund, F.; Mehrshahi, P.; Bakowski, K.; Lauersen, K. J.; Pérez-Pérez, M.-E.; Auroy, P.; Gorchs Rovira, A.; Sauret-Gueto, S. Birth of a Photosynthetic Chassis: A MoClo Toolkit Enabling Synthetic Biology in the Microalga Chlamydomonas Reinhardtii. *ACS Synth. Biol.* **2018**, *7* (9), 2074–2086. https://doi.org/10.1021/acssynbio.8b00251.
(27) Mózsik, L.; Pohl, C.; Meyer, V.; Bovenberg, R. A.; Nygård, Y.; Driessen, A. J. Modular Synthetic Biology Toolkit for Filamentous Fungi. *ACS Synth. Biol.* **2021**, *10* (11), 2850–2861. https://doi.org/10.1021/acssynbio.1c00260.
(28) Solomon, K. V.; Henske, J. K.; Theodorou, M. K.; O'Malley, M. A. Robust and Effective Methodologies for Cryopreservation and DNA Extraction from Anaerobic Gut Fungi. *Anaerobe* **2016**, *38*, 39–46. https://doi.org/10.1016/j.anaerobe.2015.11.008.
(29) Youssef, N. H.; Couger, M. B.; Struchtemeyer, C. G.; Liggenstoffer, A. S.; Prade, R. A.; Najar, F. Z.; Atiyeh, H. K.; Wilkins, M. R.; Elshahed, M. S. The Genome of the Anaerobic Fungus Orpinomyces Sp. Strain C1A Reveals the Unique Evolutionary History of a Remarkable Plant Biomass Degrader. *Appl. Environ. Microbiol.* **2013**, *79* (15), 4620. https://doi.org/10.1128/AEM.00821-13.
(30) Chen, Y.-C.; Liu, T.; Yu, C.-H.; Chiang, T.-Y.; Hwang, C.-C. Effects of GC Bias in Next-Generation-Sequencing Data on De Novo Genome Assembly. *PLOS ONE* **2013**, *8* (4), e62856. https://doi.org/10.1371/journal.pone.0062856.
(31) Orpin, C. The Rumen Flagellate Piromonas Communis: Its Life-History and Invasion of Plant Material in the Rumen. *Microbiology* **1977**, *99* (1), 107–117. https://doi.org/10.1099/00221287-99-1-107.
(32) Michielse, C. B.; Hooykaas, P. J.; van den Hondel, C. A.; Ram, A. F. Agrobacterium-Mediated Transformation as a Tool for Functional Genomics in Fungi. *Curr. Genet.* **2005**, *48* (1), 1–17. https://doi.org/10.1007/s00294-005-0578-0.
(33) Turgeon, B. G.; Condon, B.; Liu, J.; Zhang, N. Protoplast Transformation of Filamentous Fungi. In *Molecular and cell biology methods for fungi*; Springer, 2010; pp 3–19.

(34) Durand, R.; Rascle, C.; Fischer, M.; Fèvre, M. Transient Expression of the B-Glucuronidase Gene after Biolistic Transformation of the Anaerobic Fungus Neocallimastix Frontalis. *Curr. Genet.* **1997**, *31*, 158–161. https://doi.org/10.1007/s002940050190.
(35) Calkins, S. S.; Elledge, N. C.; Mueller, K. E.; Marek, S. M.; Couger, M. B.; Elshahed, M. S.; Youssef, N. H. Development of an RNA Interference (RNAi) Gene Knockdown Protocol in the Anaerobic Gut Fungus Pecoramyces Ruminantium Strain C1A. *PeerJ* **2018**, *6*, e4276–e4276. https://doi.org/10.7717/peerj.4276.
(36) Theodorou, M. K.; Davies, D. R.; Nielsen, B. B.; Lawrence, M. I.; Trinci, A. P. Determination of Growth of Anaerobic Fungi on Soluble and Cellulosic Substrates Using a Pressure Transducer. *Microbiology* **1995**, *141* (3), 671–678. https://doi.org/10.1099/13500872-141-3-671.
(37) Lee, H. B.; Kim, Y.; Kim, J. C.; Choi, G. J.; Park, S.-H.; Kim, C.-J.; Jung, H. S. Activity of Some Aminoglycoside Antibiotics against True Fungi, Phytophthora and Pythium Species. *J. Appl. Microbiol.* **2005**, *99* (4), 836–843. https://doi.org/10.1111/j.1365-2672.2005.02684.x.
(38) Chakraborty, S.; Gogoi, M.; Chakravortty, D. Lactoylglutathione Lyase, a Critical Enzyme in Methylglyoxal Detoxification, Contributes to Survival of Salmonella in the Nutrient Rich Environment. *Virulence* **2015**, *6* (1), 50–65. https://doi.org/10.4161/21505594.2014.983791.
(39) Grigoriev, I. V.; Nikitin, R.; Haridas, S.; Kuo, A.; Ohm, R.; Otillar, R.; Riley, R.; Salamov, A.; Zhao, X.; Korzeniewski, F.; Smirnova, T.; Nordberg, H.; Dubchak, I.; Shabalov, I. MycoCosm Portal: Gearing up for 1000 Fungal Genomes. *Nucleic Acids Res.* **2014**, *42* (D1), D699–D704. https://doi.org/10.1093/nar/gkt1183.
(40) Korithoski, B.; Lévesque, C. M.; Cvitkovitch, D. G. Involvement of the Detoxifying Enzyme Lactoylglutathione Lyase in Streptococcus Mutans Aciduricity. *J. Bacteriol.* **2007**, *189* (21), 7586–7592. https://doi.org/10.1128/JB.00754-07.
(41) Xu, D.; Liu, X.; Guo, C.; Zhao, J. Methylglyoxal Detoxification by an Aldo-Keto Reductase in the Cyanobacterium Synechococcus Sp. PCC 7002. *Microbiology* **2006**, *152* (7), 2013–2021. https://doi.org/10.1099/mic.0.28870-0.
(42) Varoquaux, N.; Liachko, I.; Ay, F.; Burton, J. N.; Shendure, J.; Dunham, M. J.; Vert, J.-P.; Noble, W. S. Accurate Identification of Centromere Locations in Yeast Genomes Using Hi-C. *Nucleic Acids Res.* **2015**, *43* (11), 5331–5339. https://doi.org/10.1093/nar/gkv424.
(43) Goffeau A.; Barrell B. G.; Bussey H.; Davis R. W.; Dujon B.; Feldmann H.; Galibert F.; Hoheisel J. D.; Jacq C.; Johnston M.; Louis E. J.; Mewes H. W.; Murakami Y.; Philippsen P.; Tettelin H.; Oliver S. G. Life with 6000 Genes. *Science* **1996**, *274* (5287), 546–567. https://doi.org/10.1126/science.274.5287.546.
(44) Russ C.; Lang B. F.; Chen Z.; Gujja S.; Shea T.; Zeng Q.; Young S.; Cuomo C. A.; Nusbaum C. Genome Sequence of Spizellomyces Punctatus. *Genome Announc.* **2016**, *4* (4), e00849-16. https://doi.org/10.1128/genomeA.00849-16.
(45) Baker, S. E.; Schackwitz, W.; Lipzen, A.; Martin J.; Haridas, S.; LaButti, K.; Grigoriev, I. V.; Simmons, B. A.; McCluskey, K. Draft Genome Sequence of Neurospora Crassa Strain FGSC 73. *Genome Announc.* **2015**, *3* (2), e00074-15. https://doi.org/10.1128/genomeA.00074-15.
(46) Shcherbakova, D. M.; Verkhusha, V. V. Near-Infrared Fluorescent Proteins for Multicolor in Vivo Imaging. *Nat. Methods* **2013**, *10* (8), 751–754. https://doi.org/10.1038/nmeth.2521.
(47) Lecoq, J.; Schnitzer, M. J. An Infrared Fluorescent Protein for Deeper Imaging. *Nat. Biotechnol.* **2011**, *29* (8), 715–716. https://doi.org/10.1038/nbt.1941.
(48) Lu, J.; Wu, T.; Zhang, B.; Liu, S.; Song, W.; Qiao, J.; Ruan, H. Types of Nuclear Localization Signals and Mechanisms of Protein Import into the Nucleus. *Cell Commun. Signal.* **2021**, *19* (1), 60. https://doi.org/10.1186/s12964-021-00741-y.
(49) Wilken, St. E.; Seppälä, S.; Lankiewicz, T. S.; Saxena, M.; Henske, J. K.; Salamov, A. A.; Grigoriev, I. V.; O'Malley, M. A. Genomic and Proteomic Biases Inform Metabolic Engineering Strategies for Anaerobic Fungi. *Metab. Eng. Commun.* **2020**, *10*, e00107. https://doi.org/10.1016/j.mec.2019.e00107.
(50) Shitashima, Y.; Shimozawa, T.; Asahi, T.; Miyawaki, A. A Dual-Ligand-Modulable Fluorescent Protein Based on UnaG and Calmodulin. *Biochem. Biophys. Res. Commun.* **2018**, *496* (3), 872–879. https://doi.org/10.1016/j.bbrc.2018.01.134.
(51) Wilson, F. M.; Harrison, R. J. CRISPR/Cas9 Mediated Editing of the Quorn Fungus Fusarium Venenatum A3/5 by Transient Expression of Cas9 and SgRNAs Targeting Endogenous Marker Gene PKS12. *Fungal Biol. Biotechnol.* **2021**, *8* (1), 15. https://doi.org/10.1186/s40694-021-00121-8.

(52) Foster, A. J.; Martin-Urdiroz, M.; Yan, X.; Wright, H. S.; Soanes, D. M.; Talbot, N. J. CRISPR-Cas9 Ribonucleoprotein-Mediated Co-Editing and Counterselection in the Rice Blast Fungus. *Sci. Rep.* **2018**, *8* (1), 14355. https://doi.org/10.1038/s41598-018-32702-w.
(53) Jiang, W.; Brueggeman, A. J.; Horken, K. M.; Plucinak, T. M.; Weeks, D. P. Successful Transient Expression of Cas9 and Single Guide RNA Genes in Chlamydomonas Reinhardtii. *Eukaryot. Cell* **2014**, *13* (11), 1465–1469. https://doi.org/10.1128/EC.00213-14.
(54) Henske, J. K.; Wilken, St. E.; Solomon, K. V.; Smallwood, C. R.; Shutthanandan, V.; Evans, J. E.; Theodorou, M. K.; O'Malley, M. A. Metabolic Characterization of Anaerobic Fungi Provides a Path Forward for Bioprocessing of Crude Lignocellulose. *Biotechnol. Bioeng.* **2018**, *115* (4), 874–884. https://doi.org/10.1002/bit.26515.
(55) Ranganathan, A.; Smith, O. P.; Youssef, N. H.; Struchtemeyer, C. G.; Atiyeh, H. K.; Elshahed, M. S. Utilizing Anaerobic Fungi for Two-Stage Sugar Extraction and Biofuel Production from Lignocellulosic Biomass. *Front. Microbiol.* **2017**, *8*. https://doi.org/10.3389/fmicb.2017.00635.
(56) Yıldırım, E.; Ince, O.; Aydin, S.; Ince, B. Improvement of Biogas Potential of Anaerobic Digesters Using Rumen Fungi. *Renew. Energy* **2017**, *109*, 346–353. https://doi.org/10.1016/j.renene.2017.03.021.
(57) Procházka, J.; Mrázek, J.; Štrosová, L.; Fliegerová, K.; Zábranská, J.; Dohányos, M. Enhanced Biogas Yield from Energy Crops with Rumen Anaerobic Fungi. *Eng. Life Sci.* **2012**, *12* (3), 343–351. https://doi.org/10.1002/elsc.201100076.
(58) Kumar, S.; Stecher, G.; Li, M.; Knyaz, C.; Tamura, K. MEGA X: Molecular Evolutionary Genetics Analysis across Computing Platforms. *Mol. Biol. Evol.* **2018**, *35* (6), 1547–1549. https://doi.org/10.1093/molbev/msy096.
(59) Price, M. N.; Dehal, P. S.; Arkin, A. P. FastTree: Computing Large Minimum Evolution Trees with Profiles Instead of a Distance Matrix. *Mol. Biol. Evol.* **2009**, *26* (7), 1641–1650.
(60) Wickham, H. *Ggplot2: Elegant Graphics for Data Analysis*; Springer-Verlag New York, 2016.
(61) Borchers, H. *pracma: Practical Numerical Math Functions*. https://CRAN.R-project.org/package=pracma (accessed 2022-08-04).
(62) Schindelin, J.; Arganda-Carreras, I.; Frise, E.; Kaynig, V.; Longair, M.; Pietzsch, T.; Preibisch, S.; Rueden, C.; Saalfeld, S.; Schmid, B.; Tinevez, J.-Y.; White, D. J.; Hartenstein, V.; Eliceiri, K.; Tomancak, P.; Cardona, A. Fiji: An Open-Source Platform for Biological-Image Analysis. *Nat. Methods* **2012**, *9* (7), 676–682. https://doi.org/10.1038/nmeth.2019.
(63) R Core Team. *R: A Language and Environment for Statistical Computing*. https://www.R-project.org/ (accessed 2022-07-28).
(64) Bodenhofer, U.; Bonatesta, E.; Horejš-Kainrath, C.; Hochreiter, S. Msa: An R Package for Multiple Sequence Alignment. *Bioinformatics* **2015**, *31* (24), 3997–3999. https://doi.org/10.1093/bioinformatics/btv494.
(65) Gentleman, R. C.; Carey, V. J.; Bates, D. M.; Bolstad, B.; Dettling, M.; Dudoit, S.; Ellis, B.; Gautier, L.; Ge, Y.; Gentry, J. Bioconductor: Open Software Development for Computational Biology and Bioinformatics. *Genome Biol.* **2004**, *5* (10), 1–16. https://doi.org/10.1186/gb-2004-5-10-r80.

Accepted Manuscript
Version of Record at: https://doi.org/10.1021/acssynbio.2c00502

711 **For Table of Contents Only**

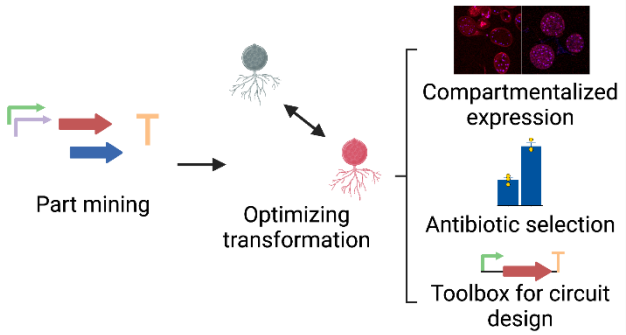

712